Journal of The Electrochemical Society, **163** (2) A19-A26 (2016)
0013-4651/2016/163(2)/A19/8/$33.00 © The Electrochemical Society

Laser-Induced Breakdown Spectroscopy of Laser-Structured $Li(NiMnCo)O_2$ Electrodes for Lithium-Ion Batteries

P. Smyrek,[a,b,z] J. Pröll,[a] H. J. Seifert,[a,*] and W. Pfleging[a,b]

[a]*Karlsruhe Institute of Technology, IAM-AWP, 76021 Karlsruhe, Germany*
[b]*Karlsruhe Nano Micro Facility, 76344 Eggenstein-Leopoldshafen, Germany*

Cathode materials such as $Li(NiMnCo)O_2$ (NMC) are presently under intense investigation regarding an improvement of lithium-ion cell cycling behavior by simultaneously providing reasonable material and manufacturing costs. Lithium-ion batteries require a further increase in cell life-time and a significant improvement in cycle stability for the use as energy storage system in high energy and high power applications such as for stationary devices and electric vehicles. Previous studies have shown that laser processing of three-dimensional (3D) micro-features in electrodes increases the active surface area and therefore the lithium-ion diffusion cell kinetics. Within this study, NMC cathodes were prepared by tape-casting and subsequent ultrafast laser-structuring. The capacity retention of lithium-ion cells with structured/unstructured NMC electrodes was measured by galvanostatic cycling at high charging/discharging currents. Furthermore, laser-induced breakdown spectroscopy (LIBS) was used for post-mortem analysis of lithium concentration in electrochemically cycled NMC cathodes based on calibration studies with electrodes at different State-of-Charges. LIBS was applied for electrochemically cycled NMC cathodes in order to investigate the degradation processes for different cell architectures (structured, unstructured). First results achieved from post-mortem studies using LIBS will be presented.
 [DOI: 10.1149/2.0981514jes]

Manuscript submitted August 26, 2015; revised manuscript received October 7, 2015. Published October 30, 2015.

During the last years, lithium nickel manganese cobalt oxide ($Li(Ni,Mn,Co)O_2$, NMC) has acquired great interest as cathode material for high-energy and high-power lithium-ion battery application.[1] NMC was first introduced by Ohzuku et al. in 2001[2,3] and since then has attained attractiveness because of its many advantages such as high energy density, high power density, high specific capacity, high rate capability and good thermal stability in the fully charged state.[4–7] However, high-energy density applications require cathode composite thick films of 100–200 μm.[8] Thick cathode layers suffer from insufficient electrolyte wetting behavior and poor cycling performance at high charging and discharging rates.[9] In order to overcome these drawbacks, recent studies focused on the development of laser-structuring processes for formation of three-dimensional (3D) micro-structures in thick-film cathodes such as $LiCoO_2$, $LiMn_2O_4$, and NMC, respectively.[10–12] It was found that 3D micro-structures can stabilize the capacity even at high charging and discharging rates due to improved lithium-ion diffusion kinetics in laser-structured cathodes. Additionally, it could be shown that 3D micro-structures in thick film tape-cast electrodes offer a fast and homogeneous wetting with liquid electrolyte in comparison to lithium-ion cells with unstructured electrodes.

Nevertheless, the investigation of lithium is quite crucial to understand the diffusion mechanisms during electrochemical reactions. Conventional analysis methods such as X-ray diffraction (XRD), X-ray fluorescence (XRF), and electron probe micro analyzer (EPMA) are insufficient to distinguish lithium.[13] Other analytical methods such as X-ray photoelectron spectroscopy (XPS), Auger electron spectroscopy (AES), and time of flight-secondary ion mass spectrometry (ToF-SIMS) have been used for the chemical characterization, however, vacuum environment is required[14] and the lithium sensitivity is quite bad for XPS or AES. Further, most of these techniques are limited due to several reasons such as restriction of sample shape or nature, long time requirement for analysis or poor resolution.[15]

Laser-induced breakdown spectroscopy (LIBS) offer the possibility to characterize the elemental composition very fast. Only one laser pulse in ambient air is required in order to assign a local State-of-Charge (SOC). Bulk analysis, depth profiling, surface element mapping as well as layer-by-layer analysis can be carried out at atmospheric pressure conditions.[16] Furthermore, LIBS is the only technique capable of performing direct 3D analysis with micrometric resolution.[17] This is an approach in order to achieve non-intrusive, qualitative and quantitative elemental analysis and can be easily appropriate for computerized analysis using fiber optics for *real-time* and in situ analysis.[18]

In this paper we describe the manufacturing and electrochemical cycling behavior of thick-film NMC electrodes and subsequent post mortem elemental characterization using LIBS. Ultrafast laser structuring processes were performed for modification and formation of 3D micro-structures in cathode materials. LIBS was used as a characterization method to determine the elemental composition in NMC cathodes at different SOC.

Experimental

Tape-casting of lithium nickel manganese cobalt oxide cathodes.— NMC composite cathodes were tape-casted onto 20 μm thick aluminum substrates using a tape-casting film coater (MSK-AFA-L800-H, MTI Corporation, USA) and subsequently dried for 2 h by using a heating lid. The cathode film was calendered applying a compact hot rolling press (Precision 4″ Hot Rolling Press/Calender, MTI Corporation, USA) with a rolling speed of 8 mm/s. The roller temperature was maintained at 50 °C. By using a doctor blade gap of 360 μm, a film thickness of 100 μm ± 3 μm could be achieved. The slurry consisted of 90 wt% of NMC (Ni:Mn:Co = 1:1:1, MTI Corporation, USA, Figure 1a) with a mean particle size of 9.89 μm (Figure 1b) and a BET surface of 0.3835 m^2/g ± 0,0029 m^2/g, 5 wt% of conductive agent (TIMCAL SUPER C65, MTI Corporation, USA), 5 wt% of polyvinylidene fluoride (PVDF) binder (MTI Corporation, USA), and N-Methyl-2-pyrrolidone (NMP) (BASF, Germany) as solvent.

Femtosecond laser-structuring.— 3D architectures in NMC were generated by using a micromachining workstation (PS450-TO, Optec, Belgium) equipped with an ultrafast fiber laser (Tangerine, Amplitude Systemes, France) operating with an average power of 20 W and a maximum pulse energy of 100 μJ at 1030 nm (TEM_{00} with $M^2 < 1.3$). The pulse duration can be tuned in the range from 330 fs up to 10 ps. The laser structuring process was performed applying a laser wavelength of 515 nm, a repetition rate of 500 kHz and an average laser power of 4.8 W. The pulse duration was set to 350 fs. The structuring process was carried out under ambient air. The ablated material was removed during the structuring process by an external exhaust which has been positioned directly in front of the sample. For generation of a free standing microstructure, the laser beam was guided through a beam expander (3-fold) and was subsequently scanned over the sample surface using a RhothorTM Laser Deflection Systems scan head (Newson Engineering BV, Belgium). The process was performed by scanning the laser beam along each line

*Electrochemical Society Active Member.
[z]E-mail: peter.smyrek@kit.edu

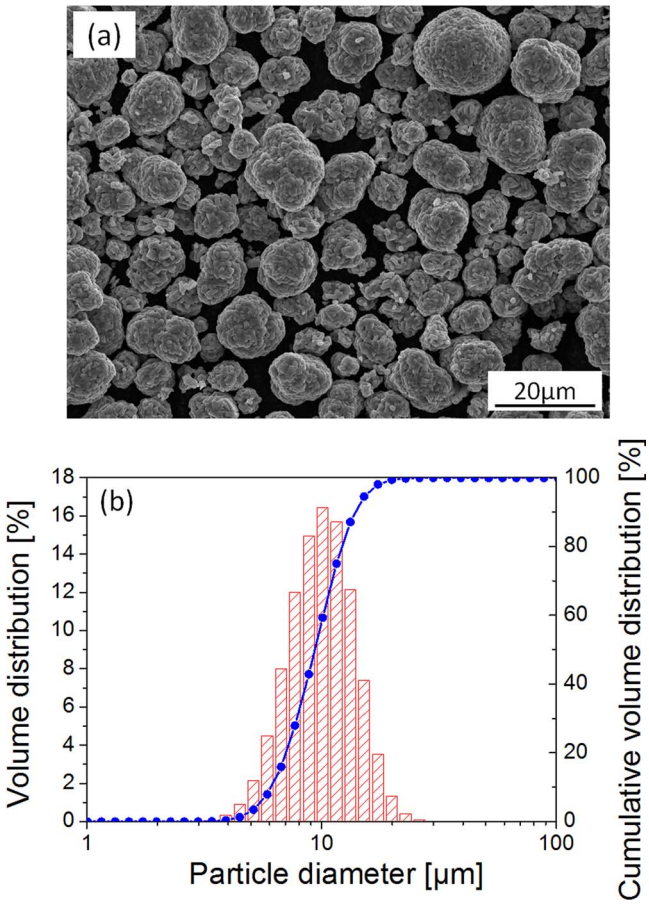

Figure 1. NMC powder analysis: (a) particle morphology of the used active powder studied by SEM, (b) measurement of particle size by Laser Scattering Particle Size Distribution Analyzer LA-950.

16 times using a f-theta lens with a focal length of 100 mm (Figure 2). The scanning velocity was set to 500 mm/s for all experiments.

Battery assembling and electrochemical characterization.— Lithium-ion Swagelok cells were assembled in an argon-filled glove box (LABmaster sp, M. Braun Inertgas-Systeme GmbH, H_2O < 0.1 ppm and O_2 < 0.1 ppm). The principle set-up of the electrochemical cell is described elsewhere.[19] The cathode material was cut by laser into circular disks with 12 mm in diameter. The cutting process was carried out using a wavelength of 515 nm, a pulse duration of 350 fs, a repetition rate of 200 kHz, a scanning velocity of 50 mm/s and an average laser power of 6 W. All cathodes were heated in a vacuum oven of type VT 6025 (Thermo SCIENTIFIC, Germany) at 130 °C for 24 h prior to the assembly process. Lithium metal (Sigma Aldrich Chemistry, USA) was used as counter electrode and the electrolyte was ethylene carbonate and dimethyl carbonate with one molar lithium hexafluorophosphate conducting salt (EC:DMC 1:1, 1M $LiPF_6$, BASF, Germany). The separator was a glass micro-fiber with a thickness of 260 µm (GF/A filter, Whatman Company). All battery tests were carried out using a BT2000 battery cycler (Arbin Instruments, USA).

In a first step, galvanostatic measurements were performed in order to determine the cell properties of uncalendered, calendered and calendered/laser-structured NMC cathodes. For this purpose, only uncalendered and calendered NMC thick film electrodes were inserted in an electrolyte bath for 1 h. Additionally, electrochemical formation was carried out with a C/10 charging and discharging rate for five cycles in a voltage range from 3.0 V – 4.2 V. Further, cyclic voltammograms were recorded for three cycles using a 0.01 mV/s scan rate and a voltage window of 3.0 V – 4.2 V. Then, the C-rate was increased from C/5 (five cycles charge and discharge) to C/2 (five cycles), 1C (ten cycles), 2C (ten cycles), and finally 3C (ten cycles). For discharging rates > C/2, the charging rate was set to C/2 (Table I).

In a second step, cyclic voltammetry (CV) and galvanostatic measurements were carried out with calendered and unstructured NMC cathodes for subsequent LIBS investigations. The voltage window for CV was 3.0 V – 5.0 V. The scan rate was maintained for three cycles at 0.01 mV/s. In addition, NMC cathodes (Cell 1 - 9) were galvanostatically charged in 0.25 V steps from 3.0 V to 5.0 V (half-cycle) using a C/20 rate and the constant current constant voltage method (CCCV) for post-mortem LIBS studies at different SOC (Table II). For this purpose the Swagelok cells were disassembled in an argon-filled glove box and the cathode layers were washed in dimethylcarbonate (DMC, Merck AG, Germany) for 60 min. After the washing procedure, the NMC electrodes were stored in a vacuum chamber for 120 min in order to remove the solvent. Furthermore, LIBS measurements were performed in order to measure the lithium concentration at different SOC.

In a third step, galvanostatic measurements were carried out in order to investigate the lithium distribution in cycled and unstructured / laser-structured NMC electrodes by using LIBS. First, an electrochemical formation was realized with a C-rate of C/10 for charging and discharging before the cells get charged and discharged by using a C-rate of C/2 and 2C in a voltage range from 3.0 V – 4.2 V. The measurement was carried out until 800 cycles were performed (Table III).

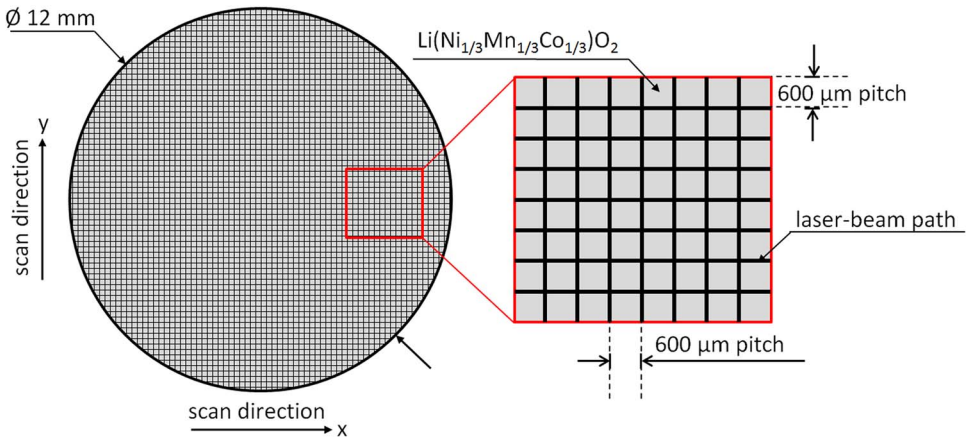

Figure 2. Schematic diagram of a tape-casted and fs laser-structured NMC thick film electrode.

Table I. Electrochemical testing procedure for Swagelok cells with uncalendered, calendered and calendered/laser-structured NMC thick films.

Cell Assembly	Electrochemical Formation	Cyclic Voltammetry	Galvanostatic Cycling				
Uncalendered NMC cathode	Charging: C/10 Discharging: C/10 Cycles: 5 Voltage Range: 3.0 V - 4.2 V	Scan rate: 0.01 mV/s Cycles: 3 Voltage Range: 3.0 V - 4.2 V	Charging: C/5 Discharging: C/5 Cycles: 5	Charging: C/2 Discharging: C/2 Cycles: 5	Charging: C/2 Discharging: 1C Cycles: 10	Charging: C/2 Discharging: 2C Cycles: 10	Charging: C/2 Discharging: 3C Cycles: 10
Calendered NMC cathode							
Calendered / laser-structured NMC cathode							

Table II. Electrochemical testing procedure for Swagelok cells with calendered and unstructured NMC thick films for LIBS investigations at different SOC.

Cell Assembly	Cyclic Voltammetry	Galvanostatic Cycling				
Calendered / unstructured NMC cathodes	Scan rate: 0.01 mV/s Cycles: 3 Voltage Range: 3.0 V - 5.0 V	Cell 1 Charging: C/20 Upper voltage: 3.0 V	Cell 2 Charging: C/20 Upper voltage: 3.25 V	Cell 3 Charging: C/20 Upper voltage: 3.5 V	Cell 4 Charging: C/20 Upper voltage: 3.75 V	Cell 5 Charging: C/20 Upper voltage: 4.0 V
		Cell 6 Charging: C/20 Upper voltage: 4.25 V	Cell 7 Charging: C/20 Upper voltage: 4.5 V	Cell 8 Charging: C/20 Upper voltage: 4.75 V	Cell 9 Charging: C/20 Upper voltage: 5.0 V	

Table III. Electrochemical testing procedure for Swagelok cells with cycled and calendered unstructured/laser-structured NMC thick films for subsequent LIBS measurements.

Cell Assembly	Electrochemical Formation	Galvanostatic Cycling
Calendered / unstructured NMC cathodes	Charging: C/10 Discharging: C/10 Cycles: 5 Voltage Range: 3.0 V - 4.2 V	Charging: C/5 Discharging: 2C Cycles: 800
Calendered / laser-structured NMC cathodes		

Laser-induced breakdown spectroscopy.— The experimental setup of LIBS is shown in Figure 3. The device can be divided into an excitation system (laser source), a detection system (type: FiberLIBS SN013, Secopta GmbH, Germany) as well as into an analytical system (Software/Analysis). A pulsed laser beam is focused onto the cathode sample surface and generates a laser-induced plasma plume. The emitted plasma light is focused onto an optical fiber which is attached to a Czerny-Turner spectrometer inside the "FiberLIBS module". The spectrometer was equipped with a ruled grating of 1200 grooves / mm blazed at 250 nm. The output end of the spectrometer was coupled with a back-thinned charge-coupled detector (CCD) including an electronic shutter function (Hamamatsu S11155). The CCD had a pixel width of 14 µm and was used to detect the dispersed light from the laser-induced plasma.

LIBS was used for investigation of cycled and calendered/laser-structured cathodes using a mode-locked diode pumped solid state (DPSS) Nd:YAG laser operating at a wavelength of 1064 nm and a maximum pulse energy of 3 mJ. The pulse duration was set to 1.5 ns. The laser repetition rate was 100 Hz. A focusing lens with focal length of 75 mm was applied and leading to a laser focus diameter of about

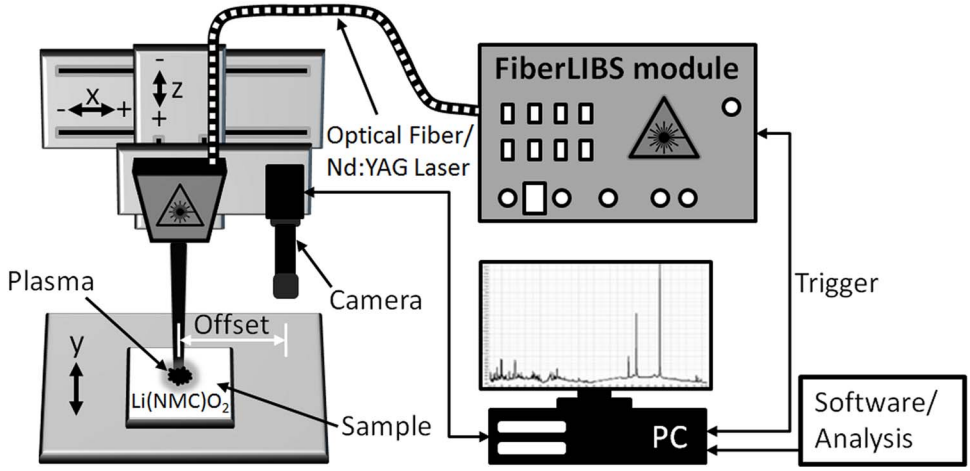

Figure 3. Scheme of the experimental setup of LIBS for the characterization of NMC electrodes.

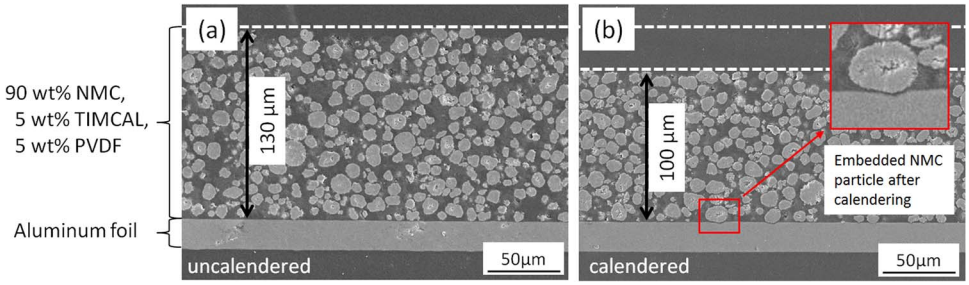

Figure 4. Cross-sectional SEM images of an uncalendered and calendered NMC cathode: (a) uncalendered electrode with a thickness of 130 ± 6 µm, (b) calendered electrode with a thickness of 100 ± 3 µm. The inset illustrates a detected, embedded NMC particle after calendaring.

100 µm. At the sample surface a laser power density of 25.47 GW/cm^2 was achieved.

Results and Discussion

Tape-casting and calendering of NMC electrodes.— NMC cathodes consisted of three constituents: active powder, conductive agent and polymeric binder. These ingredients were mixed in defined weight proportions. For achieving a controlled coating process leading to homogeneous thickness and particle density distribution, preparation of a stable and homogeneous dispersion of active material and inactive components is required.[20] In this work, the weight proportion of active and inactive components were set to 90 wt : 5 wt : 5 wt (NMC : TIMCAL : PVDF).

For manufacturing of lithium-ion electrodes, calendering is an essential step in order to improve the particle to particle contact and to improve the film adhesion to the current collector.[7] Furthermore, calendering of the electrodes can enhance volumetric energy density due to the fact that the thickness of the cathode decreases while the mass loading of the NMC active material remains constant. Additionally, calendering reduces the porosity of the electrodes which may hinder the lithium-ion migration within those electrodes.[7] A 130 ± 6 µm thick NMC cathode (Figure 4a) was chosen and it was pressed down to a film thickness of 100 µm ± 3 µm (Figure 4b). It could be shown that the NMC particle density increased while the film adhesion between the composite layer and the current collector could be improved. NMC particles, which were slightly embedded in the current collector, could be detected. One embedded NMC particle is shown in Figure 4b, inset.

The porosity of uncalendered and calendered electrodes was calculated by using the following equation:[7]

$$Porosity\ P = \frac{L - W\left(\left(\frac{C1}{D1}\right) + \left(\frac{C2}{D2}\right) + \left(\frac{C3}{D3}\right)\right)}{L} \qquad [1]$$

L is the thickness of the composite layer without current collector (aluminum foil), W is the weight per area, C1, C2 and C3 are the proportion of the active material NMC, binder PVDF and conductive additive TIMCAL SUPER C65, D1, D2 and D3 are the material densities of $Li(Ni_{1/3}Mn_{1/3}Co_{1/3})O_2$, PVDF and TIMCAL SUPER C65.[7]

For uncalendered NMC films, a porosity of 50% ± 3 % could be calculated. This value is decreased down to 35% ± 3 %, after compressing the cathodes to a defined thickness of 100 µm ± 3 µm. The values which were used in order to calculate the porosity are depicted in Table IV.

Fs-laser structuring of NMC electrodes.— For laser-structuring experiments, calendered NMC cathodes with a thickness of 100 µm ± 3 µm were used in order to generate a 3D surface structure (Figure 5). By applying appropriate laser and process parameters, the composite material could be removed down to the substrate without leaving any significant damage. Previous studies have been done in order to achieve optimized structuring conditions. Different laser-powers were used and the ablation results were analyzed by SEM and cross-section analyses. The depth of each laser generated channel was measured. By using a scanning speed of 500 mm/s, 16 repetitions of each line and applying an average laser power of 4.8 W, free standing 3D micro-pillars with a pitch distance of 600 µm could be achieved (Figures 5a,b). Additionally, the crystalline structure of NMC was checked by performing XRD measurements. The XRD data (not shown here) reveal that no impurity phases or phase changes could be detected compared to unstructured NMC electrodes after laser structuring.

Figure 5c shows a cross section image of a laser-structured electrode. In comparison to ablation studies using nanosecond laser pulses,[10] the aspect ratio AR (channel depth divided by channel width at half height) of the generated grooves could be increased by a factor of five, leading to a value of AR = 13. The influence of fs-laser structured 3D architectures in NMC thick films during electrochemical cycling is discussed and presented in Battery testing section.

Battery testing.— Galvanostatic cycling was carried out for as-deposited (130 µm ± 6 µm thickness), calendered (100 µm ± 3 µm thickness) and calendered/laser-structured (100 µm ± 3 µm thickness) NMC tape-casted electrodes (Figure 6). Electrochemical formation was performed using a charging/discharging rate of C/10 for five cycles. Afterwards, the C-rate was continuously enhanced up to 3C. For a 3C rate, the uncalendered NMC cathode exhibited worst capacity retention compared to all other cathodes (calendered, calendered/laser-structured) (Figure 6). It is assumed that this is due

Table IV. Values for porosity calculation (Equation 1). (a) C1, C2, C3 (weight proportion of active powder NMC, binder PVDF, conductive additive TIMCAL), (b) D1, D2, D3 (material density of active powder NMC, binder PVDF, conductive additive TIMCAL), (c) L (real thickness of uncalendered and calendered NMC thick film), (d) W (weight per area without current collector).

Material	C1, C2, C3	D1, D2, D3	L	W
$Li(Ni_{1/3}Mn_{1/3}Co_{1/3})O_2$	90 wt%	4.68 g/cm^3[37]	thickness calendered: 100 µm ± 3 µm	
PVDF	5 wt%	1.78 g/cm^3[37]		0.02634 g/cm^2 ± 0.000672 g/cm^2
TIMCAL SUPER C65	5 wt%	1.8 g/cm^3 [MTI Corporation, USA]	thickness uncalendered: 130 µm ± 6 µm	

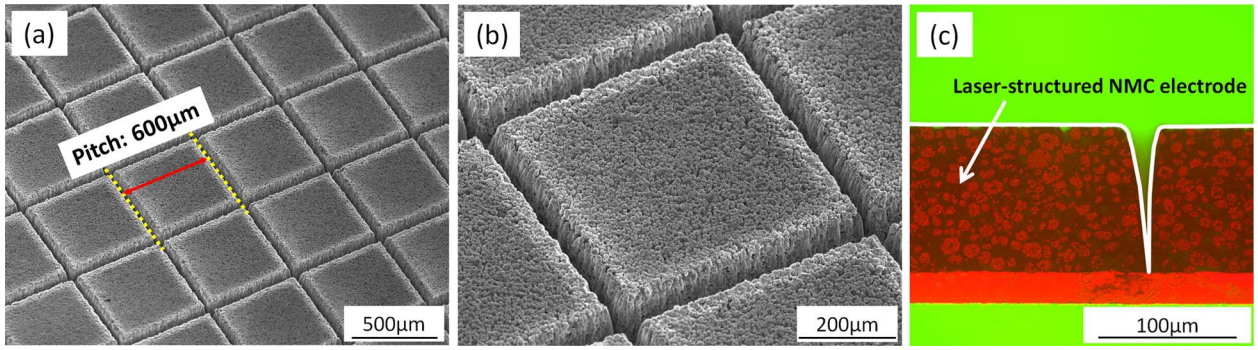

Figure 5. SEM- and microscope images of calendered and laser-structured NMC cathodes: (a,b) top-view (SEM), (c) cross-section (microscope).

to the fact that the particle - particle contact is not adjusted appropriately in order to achieve best possible conditions regarding electrical conductivity. Furthermore, within thick cathode layers (> 50 µm) the internal resistance will increase and electrolyte penetration ability will decrease. Thus, an appropriate low porosity is essential for adequate electrochemical cyclability, especially at high charging and discharging rates. Within previous studies, laser-structuring experiments have been carried out for thick-film cathodes composed of $LiMn_2O_4$ and NMC.[10] It could be shown that laser-induced 3D micro structures significantly improve the electrolyte wetting and act as an "artificial porosity" enabling electrochemical activation of active particles in deeper film layers. A similar observation could be made within this study. The most stable cycling behavior was observed for cells with calendered/laser-structured electrodes, since those electrodes provides both, improved electrical contact and an artificial porosity due to calendering and 3D laser-structuring, respectively. The capacity loss at 3C was approximately 51% while the uncalendered and calendered samples showed a capacity loss of 60% - 75%. In a recently published work of Chien-Te Hsieh et al.,[21] $LiNi_{1/3}Co_{1/3}Mn_{1/3}O_2$ electrodes were synthesized by a chemical-wet synthesis route. The layers had a thickness of around 100 µm, which is comparable with our NMC electrodes (100 µm ± 3 µm). For a voltage window of 2.8 V – 4.5 V Chien-Te Hsieh et al. achieved capacities for 1C and 2C which are similar to the capacities which were achieved in our studies (voltage window 3.0 V – 4.2 V) for calendered and unstructured NMC thick films. Furthermore, in[21] a capacity drop of around 2.5% after the first 10 cycles was observed. In our study we could achieve a slightly improved capacity retention for calendered and unstructured NMC electrodes with a capacity drop of 1.2% within the first 10 cycles. Due to laser processing, a further improvement of capacity and capacity retention for high C-rates was finally achieved. For cells with laser-structured electrodes no capacity loss was measured for the first 10 cycles at 1C (Figure 6).

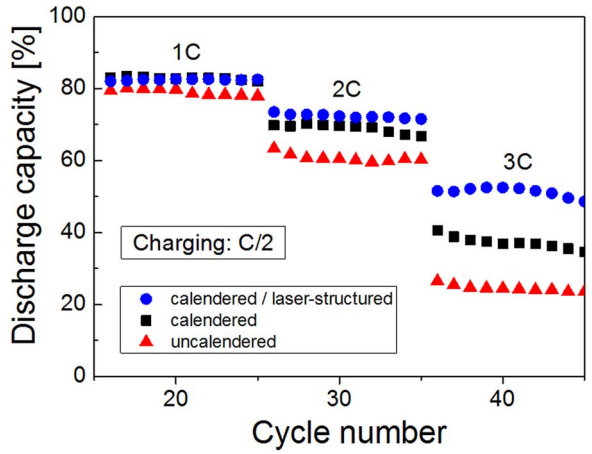

Figure 6. Discharge capacities [%] for as-deposited, calendered and calendered/laser-structured NMC cathodes.

Laser-induced breakdown spectroscopy.— LIBS was performed in order to detect the lithium concentration in calendered and laser-structured NMC cathodes with a thickness of 100 µm ± 3 µm. For this purpose a calibration of LIBS using NMC samples with defined Li concentration was necessary. Those samples were produced by electrochemical titration. CV and galvanostatic measurements were carried out in a broad voltage window as shown in Figure 7. By analyzing the redox pairs (Ni^{2+}/Ni^{4+}, Co^{3+}/Co^{4+}) out from CV data it could be observed that lithium deintercalation from the host lattice mainly occurs at about 3.75 V and 4.6 V, respectively (Figure 7a).

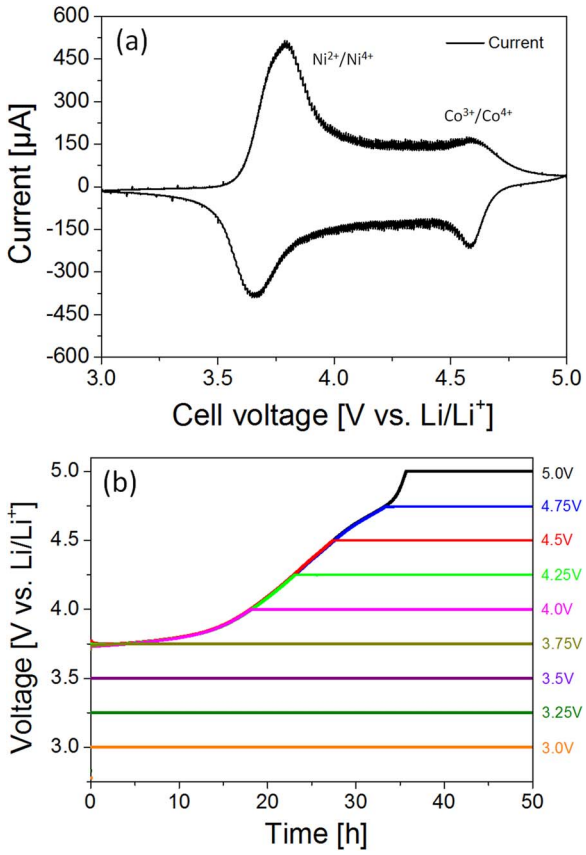

Figure 7. Cells with calendered NMC cathodes: (a) Cyclic voltammogram obtained at 2nd scan between 3.0 V and 5.0 V (vs. Li) at room temperature. The scan rate was set to 0.01 mV/s. (b) galvanostatic cycling data of nine different cells - all incorporating the same cathode constitution - at various voltages (3.0 V – 5.0 V). Lithium metal acts as counter electrode.

Furthermore, the CV data indicate that complete lithium deintercalation can be achieved by electrochemical cycling of the cell up to a voltage of 5.0 V. For this reason, galvanostatic cycling of nine individual cells – all incorporating the same cathode constitution – was performed up to 3.0 V, 3.25 V, 3.5 V, 3.75 V, 4.0 V, 4.25 V, 4.5 V, 4.75 V and 5.0 V, respectively. This strategy was applied in order to create nine NMC electrodes (calendered/unstructured) with different SOC (Figure 7b). Those samples act as standard sample for subsequent LIBS calibration. Due to the fact that electrolyte decomposition may occur at voltages ∼ 4.6 V,[22] in each case, the electrical current was recorded during electrochemical titration. It could be observed that the current increases after 60–80 hours which can be assigned to electrolyte decomposition. In order to avoid a significant influence due to electrolyte decomposition the cells were held at the pre-set voltages for 50 hours. Integral chemical analysis (ICP-OES) of NMC electrodes cycled in this way show that galvanostatic titration up to 5.0 V leads to a complete delithiation of the cathode material.

After reaching a defined voltage through galvanostatic charging (Figure 7b), the cells were disassembled and the cathodes were washed two times for each 30 minutes in fresh DMC in an argon-filed glovebox. Then cathode layers were analyzed by LIBS. Lithium element mapping was performed in order to check whether lithium-ions could be deintercalated homogeneously from the cathode surfaces within the applied cutoff voltages. LIBS spectra were recorded after each pulse. Twelve different positions on the cathode surface were analyzed while the number of laser pulses was increased from a single shot ("measurement location 1") up to 12 laser pulses ("measurement location 12"). For each measurement location, two laser pulses were applied as cleaning step in advance. Furthermore, for each measurement location, the LIBS spectrum resulting from the third laser pulse was recorded (Figure 8a). Additionally, an evaluation software (SEC Viewer, Single Line Analysis - Editor, Secopta GmbH, Germany) was used in order to determine the peak intensity of the lithium emission line Li I (center wavelength 610.4 nm) for each measurement location. It could be shown that the Li I emission line intensity and therefore the lithium concentration at the cathode surface decreases with increasing cut-off-voltage which in turn corresponds to an increasing SOC (Figure 8b). The individual data points in Figure 8b were each calculated from 12 measurement locations at different SOC (3.0 V – 5.0 V). The error bars correspond to the standard deviation. These results clearly indicate that LIBS is suitable for investigation of element distribution within cycled cathode films.

In a further step, LIBS measurements were carried out in order to investigate the lithium distribution and a related "local State-of-Charge[c]" (SOC_{local}) in cycled and unstructured/laser-structured NMC thick films. For this purpose, electrochemical formation was carried out using a charging/discharging rate of C/10 for five cycles. Afterwards, galvanostatic measurements were performed using C-rates for charging and discharging of C/5 and 2C (Table III). After 800 cycles, the cells were disassembled in an argon-filled glove-box. The cathodes were washed two times for each 30 minutes in fresh DMC.

LIBS measurements were performed at the surface of each NMC electrode by applying a dot matrix with a point-to-point distance of 100 μm. The laser pulse energy was 3 mJ with a pulse length of 1.5 ns. The measurement area at the sample surface was adjusted to 5 mm × 5 mm. LIBS spectra were recorded for each 51×51 = 2601 measurement locations at the sample surface. Additionally, a calibration-file was generated in order to enable a mapping of the SOC_{local} of cycled and unstructured/laser-structured NMC thick films. For this purpose, a calibration model was created applying a Partial Least Square Regression Model (Partial Least Square regression, PLS-R).[23] Post-mortem results for cycled and unstructured electrodes after 800 cycles are depicted in Figure 9. It could be clearly demonstrated that the cycled and unstructured electrode show an inhomogeneous SOC_{local} distribution at the sample surface after 800 cycles (Figure 9a).

[c]SOC_{local} is a new definition in order to illustrate local inhomogeneities on electrodes which might be relevant starting points for enhanced cell degradation.

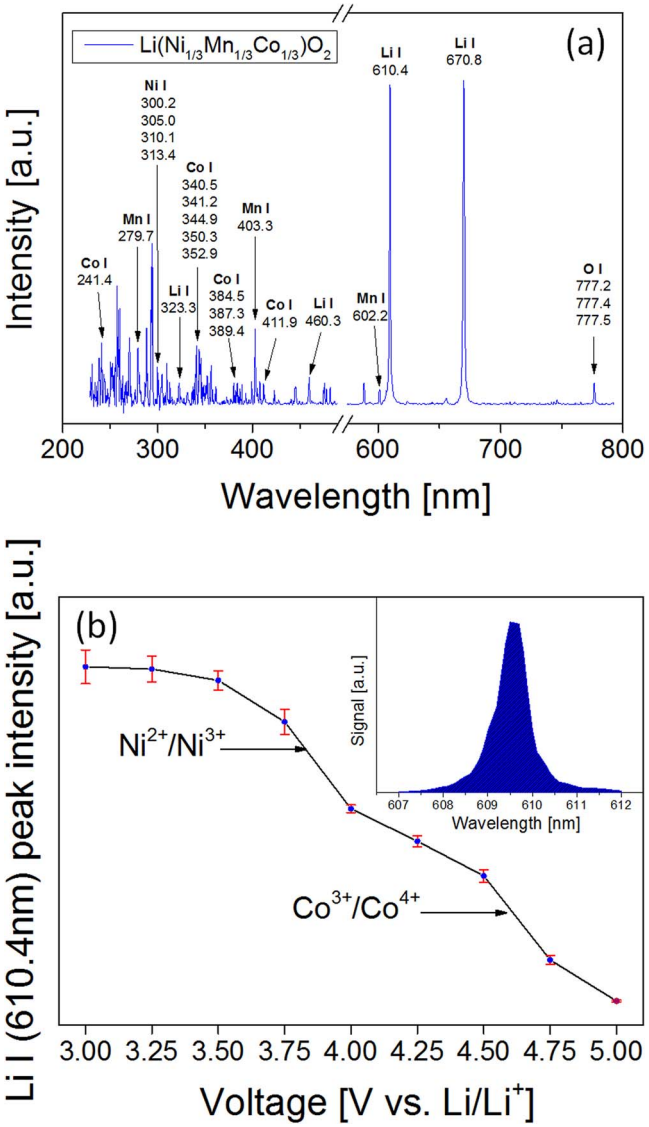

Figure 8. LIBS data of NMC thick films: (a) LIBS spectrum of a cycled (SOC 3.0 V) and calendered NMC thick film electrode resulting from the third laser pulse, (b) averaged lithium peak intensity at different SOC (3.0 V - 5.0 V).

For X = 0.1 mm – 1.5 mm and Y = 0.1 mm – 5.1 mm the SOC_{local} significantly increased and voltages larger than 4.0 V were reached. A possible cause for this inhomogeneity in voltage distribution might be an insufficient electrolyte wetting of the electrode. As mentioned before, both, a well-defined porosity and very good wetting properties are quite necessary for adequate electrochemical cyclability, especially for calendered NMC thick films at high charging/discharging C-rates. Areas which correspond to a high SOC_{local} (red areas, Figure 9a) reveal a significant drop of lithium content (red areas, Figure 9b). Electrode surfaces with inhomogeneous lithium distribution could lead to different electrical current densities during electrochemical cycling which in turn would force the chemical degradation process leading finally to a spontaneous cell failure.

For cycled and laser-structured NMC thick films, LIBS measurements were performed in order to investigate the lithium distribution and the related SOC_{local} in free standing 3D micro-structures (Figure 10). A periodic SOC distribution could be detected while an increased SOC_{local} is measured in the center of each micro-structure (Figure 10a). Additionally, it could be shown that this increase in SOC_{local} corresponds to a higher lithium amount along the edges of the free standing 3D micro-structures in comparison to the center of

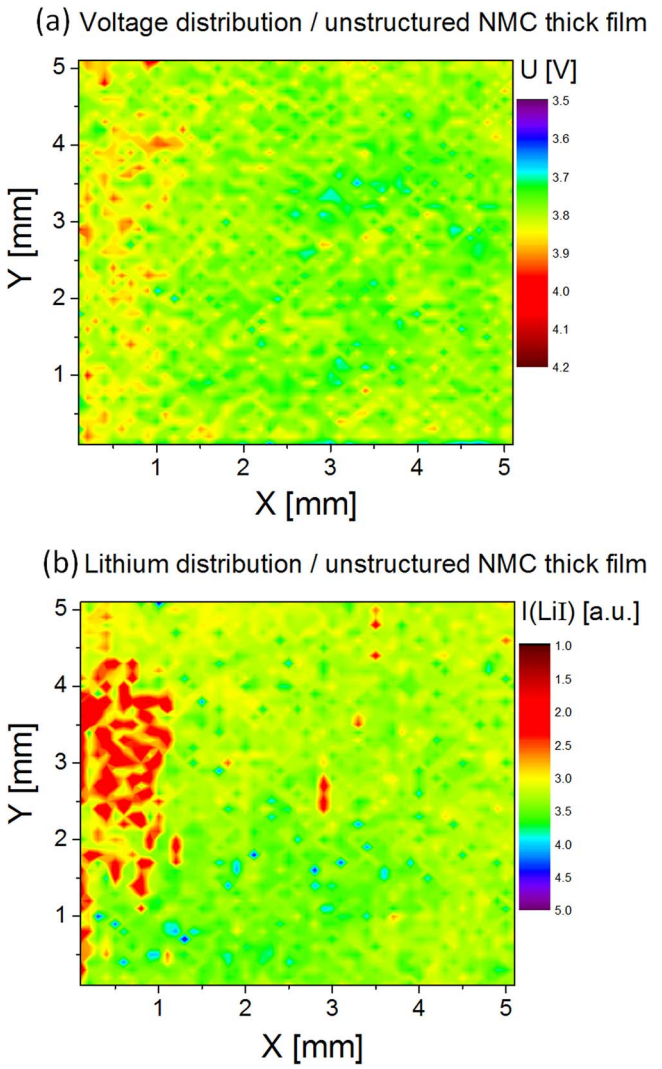

Figure 9. LIBS mapping of a cycled and unstructured NMC cathode: (a) voltage U distribution (ref. Figure 8b), (b) lithium distribution (qualitative) based on normalized peak intensity I of Li (610 nm).

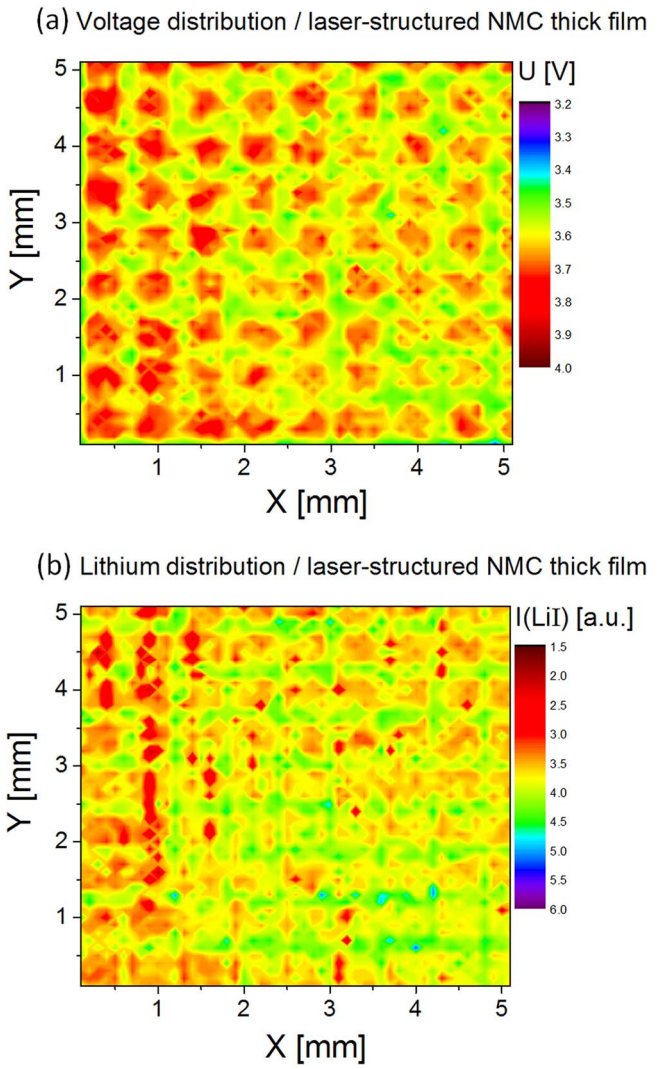

Figure 10. LIBS mapping of a cycled and laser-structured NMC cathode: (a) voltage U distribution (ref. Figure 8b), (b) lithium distribution (qualitative) based on normalized peak intensity I of Li (610 nm).

a micro structure (Figure 10b). The increased active surface area provides new pathways for lithium-ion diffusion. It seems that especially for high C-rates this becomes an important issue leading to a measurable local variation of lithium distribution on the surface of each micro-pillar. That means for high C-rates the amount of lithium intercalation along the sidewalls of each micro-pillar might increase as depicted schematically in Figure 11. Due to the fact that the electrochemical high C-rate performance is mainly influenced by the lithium-ion diffusion kinetics within the active material and the electrolyte,[8] laser-structured electrodes improve the capacity retention and finally the electrochemical performance.

Conclusions

In this study, lithium nickel manganese cobalt oxide (NMC) thick-films were deposited on 20 µm thick aluminum substrates. The as-deposited cathodes were calendered and subsequently laser-structured by using femtosecond laser radiation. 3D architectures (micro-pillars) were generated in calendered cathode films in order to improve the electrochemical performance. As-deposited, calendered and calendered/laser-structured tape-casted NMC cathodes were electrochemical investigated by galvanostatic measurements. It was demonstrated, that calendered/laser-structured cathodes offer improved capacity retention at C-rates of 1C to 3C compared to as-deposited and calendered films. This enhanced performance was assigned to the combination of calendering and laser-induced increased surface area (artificial porosity) of the cathodes allowing improved lithium-ion diffusion kinetics. Within further experiments, as-deposited and calendered NMC cathodes were analyzed by LIBS in order to investigate the elemental lithium distribution at the surface for different cutoff voltages (3.0 V, 3.25 V, 3.5 V, 3.75 V, 4.0 V, 4.25 V, 4.5 V, 4.75 V and 5.0 V). It could be demonstrated that the

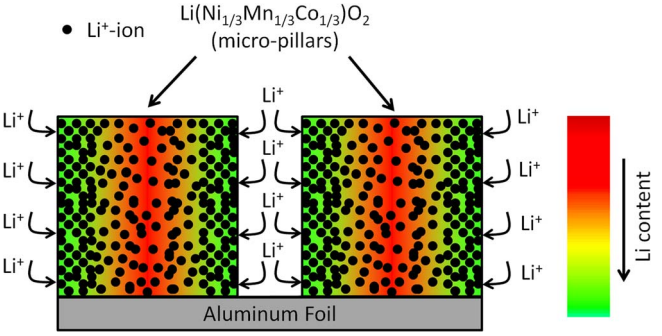

Figure 11. Schematic view of a model for laser-structured NMC electrodes during electrochemical cycling at high discharge C-rates.

lithium concentration at the surface drops down with increasing the upper cutoff voltage and, therefore, with increasing the degree of delithiation. Further, LIBS measurements were carried out on cycled and unstructured/laser-structured NMC thick films in order to determine the lithium distribution and a related SOC_{local} at the sample surface (*post-mortem*). For cycled and unstructured NMC thick films, it could be demonstrated that the SOC_{local} and lithium distribution exhibit inhomogeneous areas at the sample surface. This might be due to inhomogeneous electrolyte wetting which can lead to a rapid degradation of active particles and finally to a spontaneous cell failure. For the first time, cycled and laser-structured NMC thick films were measured post-mortem by using LIBS in order to investigate the lithium distribution in 3D micro-structures. It could be shown that the lithium content locally increases at the contours of the generated micro-pillars. We assume that due to an increase of active surface area new Li-ion path-ways were generated which are significantly activated at high charging/discharging C-rates.

Acknowledgment

We are grateful to our colleague H. Besser for his technical assistance during laser material processing. This work has been financially supported by "FabSurfWar - Design and Fabrication of Functional Surfaces with Controllable Wettability, Adhesion and Reflectivity" (Funded under: H2020-EU.1.3.3, project reference: 644971) from the European Commission under Horizon 2020 Programme (H2020). We would like to thank the Helmholtz Association for technical and staff assistance in frame the "Helmholtz-Portfolio" programme about reliability and integration of battery systems (http://www.stn.kit.edu/projects_414.php). Finally, the support for laser processing by the Karlsruhe Nano Micro Facility (KNMF, http://www.knmf.kit.edu/) a Helmholtz research infrastructure at the Karlsruhe Institute of Technology (KIT) is gratefully acknowledged.

References

1. S. H. Park, H. S. Shin, S. T. Myung, C. S. Yoon, K. Amine, and Y. J. Sun, *Chem. Mater.*, **17**, 6 (2005).
2. T. Ohzuku and Y. Makimura, *Chem. Lett.*, **30**, 642 (2001).
3. N. Yabuuchi and T. Ohzuku, *J. Power Sources*, **119**, 171 (2003).
4. J. M. Kim and H. T. Chung, *Electrochim. Acta*, **49**, 937 (2004).
5. D. C. Li, Y. Kato, K. Kobayakawa, H. Noguchi, and Y. Sato, *J. Power Sources*, **160**, 1342 (2006).
6. J. T. Xu, S. L. Chou, Q. F. Gu, H. K. Liu, and S. X. Dou, *J. Power Sources*, **225**, 172 (2013).
7. H. H. Zheng, L. Tan, G. Liu, X. Y. Song, and V. S. Battaglia, *J. Power Sources*, **208**, 52 (2012).
8. S.-L. Wu, W. Zhang, X. Song, A. K. Shukla, G. Liu, V. Battaglia, and V. Srinivasan, *J. Electrochem. Soc.*, **159**, A438 (2012).
9. O. Wollersheim and W. Pfleging, *ATZelektronik worldwide*, **7**, 38 (2012).
10. W. Pfleging and J. Pröll, *J. Mater. Chem. A*, **2**, 14918 (2014).
11. J. Pröll, H. Kim, A. Piqué, H. J. Seifert, and W. Pfleging, *J. Power Sources*, **255**, 116 (2014).
12. R. Kohler, J. Proell, M. Bruns, S. Ulrich, H. J. Seifert, and W. Pfleging, *Appl. Phys. A*, **112**, 77 (2013).
13. H. Takahara, M. Shikano, and H. Kobayashi, *J. Power Sources*, **244**, 252 (2013).
14. V. Zorba, J. Syzdek, X. Mao, R. E. Russo, and R. Kostecki, *Appl. Phys. Lett.*, **100**, 234101 (2012).
15. H. A. Ardakani and S. H. Tavassoli, *Spectrochim. Acta, Part B*, **65**, 210 (2010).
16. H. Hou, L. Cheng, T. Richardson, G. Chen, M. Doeff, R. Zheng, R. Russo, and V. Zorba, *J. Anal. At. Spectrom.*, **30**, 2295 (2015).
17. J. M. Vadillo and J. J. Laserna, *Spectrochim. Acta, Part B*, **159**, 147 (2004).
18. L. Peng, D. Sun, M. Su, J. Han, and C. Dong, *Opt. Laser Technol.*, **44**, 2469 (2012).
19. H. Kim, J. Proell, R. Kohler, W. Pfleging, A. Piqué, and J. Laser, *Micro/Nanoeng.*, **7**, 320 (2012).
20. W. Bauer and D. Nötzel, *Ceram. Int.*, **40**, 4591 (2014).
21. C.-T. Hsieh, C.-Y. Mo, Y.-F. Chen, and Y.-J. Chung, *Electrochim. Acta*, **106**, 525 (2013).
22. L. Zhang, Y. Ma, X. Cheng, P. Zuo, Y. Cui, T. Guan, C. Du, Y. Gao, and G. Yin, *Solid State Ionics*, **263**, 146 (2014).
23. W. Kessler, *Multivariate Datenanalyse für die Pharma-, Bio- und Prozessanalytik*, Wiley, Weinheim (2007).